Inorg. Chem. **2004**, *43*, 7934–7944

Forum

Folding, Conformational Changes, and Dynamics of Cytochromes *c* Probed by NMR Spectroscopy

Kara L. Bren,* Jason A. Kellogg, Ravinder Kaur, and Xin Wen

Department of Chemistry, University of Rochester, Rochester, New York 14627

Received August 5, 2004

NMR spectroscopy has become a vital tool for studies of protein conformational changes and dynamics. Oxidized Fe(III)cytochromes *c* are a particularly attractive target for NMR analysis because their paramagnetism ($S = {}^1/_2$) leads to high ^{1}H chemical shift dispersion, even for unfolded or otherwise disordered states. In addition, analysis of shifts induced by the hyperfine interaction reveals details of the structure of the heme and its ligands for native and nonnative protein conformational states. The use of NMR spectroscopy to investigate the folding and dynamics of paramagnetic cytochromes *c* is reviewed here. Studies of nonnative conformations formed by denaturation and by anomalous in vivo maturation (heme attachment) are facilitated by the paramagnetic, low-spin nature of native and nonnative forms of cytochromes *c*. Investigation of the dynamics of folded cytochromes *c* also are aided by their paramagnetism. As an example of this analysis, the expression in *Escherichia coli* of cytochrome c_{552} from *Nitrosomonas europaea* is reported here, along with analysis of its unusual heme hyperfine shifts. The results are suggestive of heme axial methionine fluxion in *N. europaea* ferricytochrome c_{552}. The application of NMR spectroscopy to investigate paramagnetic cytochrome *c* folding and dynamics has advanced our understanding of the structure and dynamics of both native and nonnative states of heme proteins.

Cytochromes *c* (cyt's *c*) were among the first proteins used in biophysical studies of protein denaturation,[1] conformational changes,[2] and conformational dynamics.[3] Despite decades of work on these proteins, their study continues to offer surprises while teaching us general lessons on protein structure and folding. The focus of this contribution to the Metalloprotein Folding Forum is the application of NMR spectroscopy to probe relationships between heme−ligand interactions, folding, and dynamics of prokaryotic and eukaryotic ferricyt's *c*. In recent years, use of NMR spectroscopy as a probe of ferricyt *c* folding and dynamics has aided analysis of folding intermediates[4,5] and identified unique dynamical properties of the heme axial Met in one cytochrome.[6] As an example of the use of NMR spectroscopy to investigate heme ligand dynamics, data on *Nitrosomonas europaea* (*Ne*) ferricyt c_{552}, a cytochrome *c* with an unusual heme electronic structure, are presented.

Cytochromes *c*

Cyt's *c* are heme-containing electron-transfer proteins found in a wide variety of eukaryotic and prokaryotic organisms.[7,8] The distinguishing feature of *c*-type cytochromes is the presence of a heme group covalently linked to the polypeptide via two (rarely, one) thioether bonds to a Cys−X−X−Cys−His motif, where His is a heme axial ligand (Figure 1). Class I cyt's *c*, the focus of this article, are small, soluble, monomeric proteins with His-Met heme

* To whom correspondence should be addressed. E-mail: bren@chem.rochester.edu.

(1) (a) Myer, Y. P. *Biochemistry* **1968**, *7*, 765−776. (b) Stellwagen. E. *Biochemistry* **1968**, *7*, 2893−2898.
(2) Theorell, H.; Åkesson, Å. *J. Am. Chem. Soc.* **1941**, *63*, 1812−1818.
(3) Ulmer, D. D.; Kägi, J. H. R. *Biochemistry* **1968**, *7*, 2710−2717.
(4) Russell, B. S.; Melenkivitz, R.; Bren, K. L. *Proc. Natl. Acad. Sci. U.S.A.* **2000**, *97*, 8312−8317.
(5) Russell, B. S.; Bren, K. L. *J. Biol. Inorg. Chem.* **2002**, *7*, 909−916.
(6) Zhong, L.; Wen, X.; Rabinowitz, T. M.; Russell, B. S.; Karan, E. F.; Bren, K. L. *Proc. Natl. Acad. Sci. U.S.A.* **2004**, *101*, 8637−8642.
(7) Moore, G. R.; Pettigrew, G. W. *Cytochrome c: Evolutionary, Structural and Physicochemical Aspects*; Springer-Verlag: New York, 1990; p 15.
(8) Scott, R. A.; Mauk, A. G. *Cytochrome c: A Multidisciplinary Approach*; University Science Books: Sausalito, CA, 1996.

10.1021/ic048925t CCC: $27.50
Published on Web 10/22/2004

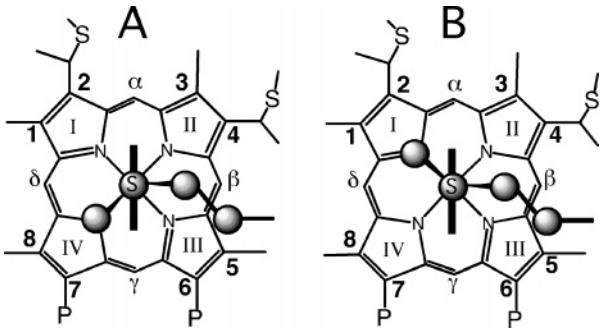

Figure 1. Heme *c* with numbering system used in text. The Cys−X−X−Cys−His heme-binding motif add to vinyl groups at heme positions 2 and 4 to form thioether linkages. The typical axial methionine side-chain orientations in (A) *Pa* cyt c_{551}, representative of the cyt's c_8, and (B) horse cyt *c*, representative of the mitochondrial cyt's *c*, are illustrated. The typical axial His ring-plane orientation in cyt's *c* is denoted with a thick line. P indicates propionate.

axial ligation, rendering the iron low-spin in both the Fe(III) ($S = {}^1/_2$) and Fe(II) ($S = 0$) oxidation states.[7,8] With some exceptions, class I cyt's *c* share similar topologies (Figure 2). Most class I cyt's *c* have four helices, including contacting N- and C-terminal helices, with the N-terminal helix exposed to solvent and the C-terminal helix more buried and forming part of the protein core. The remainder of the structure consists of loops and coils. Loop 1 contains the axial His ligand and the two Cys residues that form thioether linkages to the heme. Loop 3 is a long J-shaped loop that forms a flap over the heme face and donates the axial Met to the heme.

Being highly soluble and often displaying reversibility in unfolding, cyt's *c* have long been favorite model proteins for folding studies.[8,9] The heme *c* group also makes them attractive subjects as it serves as an endogenous spectroscopic probe of folding that remains bound to the polypeptide in the unfolded state.[8,9] Cyt *c* folding was revealed to be a unique bioinorganic problem in 1971 when it was reported that unfolding of horse ferricyt *c* is accompanied by exchange of its heme axial Met for one or more protein-donated strong-field ligands, maintaining a low-spin heme.[10] Since that initial report, heme−ligand interactions have been utilized in a range of studies for probing and manipulating cyt *c* folding and dynamics. The reader is referred to articles by Winkler and Gray (pp 7953−7960) and Turano (pp 7945−7952) in this issue for additional information on cyt *c* folding.

NMR Spectroscopy of Paramagnetic Cyt's *c*

The oxidized ($S = {}^1/_2$) state of cyt's *c* has proven attractive for NMR studies because it displays well-resolved hyperfine-shifted resonances easily detected in 1-D spectra.[11] Indeed, ferricyt *c* was the first protein for which multiple well-resolved NMR signals were detected (in 1962).[12] The prominent features of NMR spectra of ferricyt's *c* are

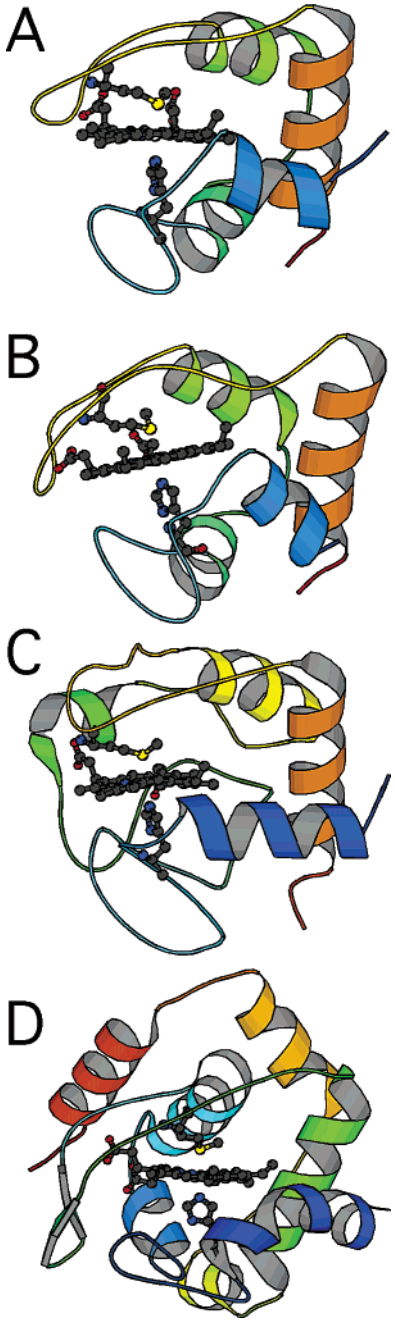

Figure 2. Structures of representative class I cyt's *c*: (A) *Pa* cyt c_{551} (PDB code 351c),[64] (B) *N. europaea* cyt c_{552} (1A56),[72] (C) horse heart cyt *c* (1HRC),[82] (D) *T. thermophilus* cyt c_{552} (1C52).[83] The structures are color-coded blue to red from the N- to C-terminus. *Ht* cyt c_{552} (1AYG), not shown, has a structure similar to A and B.[71] The loop that donates the axial Met to the heme (top as oriented) is yellow in A−C and green in D. The topology of *Tt* cyt c_{552} deviates from that shown by other class I cyt's *c*, as it contains a β-sheet and a C-terminal extension with two additional helices relative to the other cytochromes. Figures prepared using Molscript.[84]

(typically) two to four intense, well-resolved downfield-shifted resonances that are relatively narrow (for a paramagnetic molecule; Figure 3) because of the rapid relaxation for the unpaired electron from the low-spin Fe(III) center.[11] These resonances are attributed to methyl groups on the heme macrocycle (at positions 1, 3, 5, and 8; Figure 1). The shifts of the heme methyls are determined by the heme electronic structure, which in turn is related to the details of the structure of the heme and its axial ligands. To extract this information,

(9) Winkler, J. R. *Curr. Opin. Chem. Biol.* **2004**, *8*, 169−174.
(10) Babul, J.; Stellwagen, E. *Biopolymers* **1971**, *10*, 2359−2361.
(11) La Mar, G. N.; Satterlee, J. D.; de Ropp, J. S. In *The Porphyrin Handbook*; Kadish, K. M., Smith, K. M., Ruilard, R., Eds.; Academic Press: New York, 2000; Vol. 5, pp 185−298.
(12) Kowalsky, A. *J. Biol. Chem.* **1962**, *237*, 1807−1819.

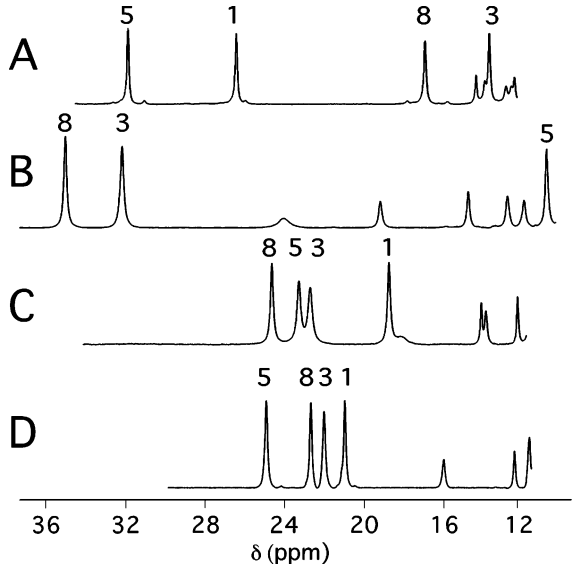

Figure 3. Downfield regions of ^{1}H NMR spectra of oxidized (A) recombinant *Pseudomonas aeruginosa* cyt c_{551},[6] (B) horse cyt *c*,[4] (C) recombinant *Hydrogenobacter thermophilus* cyt c_{552},[6] and (D) recombinant *Nitrosomonas europaea* cyt c_{552} (298 K, this work). Heme methyl resonance assignments,[24,25,85,86] using the numbering system indicated in Figure 1, are shown. Note that the heme methyl shifts in C and D are approximately averages of those in A and B; see text for discussion.

one must consider a sum of contributions to the observed shifts of a nucleus in a paramagnetic molecule (δ_{obs})

$$\delta_{obs} = \delta_{dia} + \delta_{para} = \delta_{dia} + \delta_{con} + \delta_{pc} \quad (1)$$

where δ_{dia} is the shift of the nucleus in an isostructural diamagnetic molecule and δ_{para} is the contribution to the shift from the unpaired electron−nucleus interaction.[11,13,14] In turn, δ_{para} is composed of contact (through-bond, δ_{con}) and pseudocontact (through-space, δ_{pc}) components. Because of the effective delocalization of the unpaired electron from the iron to the β-pyrrole substituents of the porphyrin group,[11,15] the δ_{con} contribution, which results from unpaired electron spin density at the resonant nucleus, is significant for the heme methyl shifts in ferricyt's *c*. Assuming a single spin state, δ_{con} is described by[11,13,14]

$$\delta_{con} = (2\pi A/h)\left[\frac{g\beta S(S+1)}{3kT\gamma}\right] \quad (2)$$

where $2\pi A/h$ is the hyperfine coupling constant for the nucleus, g is the average g value, β is the Bohr magneton, γ is the nuclear magnetogyric ratio, S is the total electron spin, k is the Boltzmann constant, and T is the absolute temperature. The pseudocontact (or dipolar) contribution (eq 3) to the hyperfine shift depends on the position of the nucleus (in polar coordinates, r, θ, Ω) with respect to the principal axes of the magnetic susceptibility tensor χ and the magnetic anisotropy (axial, $\Delta\chi_{ax}$, and rhombic, $\Delta\chi_{rh}$) of the system[11,14]

$$\delta_{pc} = (12\pi\mu_0 N_A r^3)^{-1}[\Delta\chi_{ax}(3\cos^2\theta - 1) + {}^3/_2\Delta\chi_{rh}(\sin^2\theta\cos 2\Omega)] \quad (3)$$

Both the contact and pseudocontact shifts are intimately related to the type and orientation of the heme axial ligands.

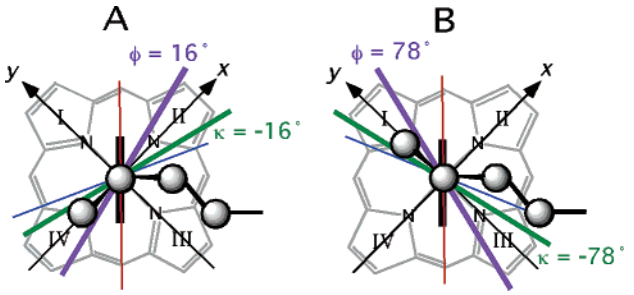

Figure 4. Representation of the counterrotation rule, which states that the effective axial ligand plane angle (Φ) is related to the orientation of the χ_{xx} axis (κ) according to $\kappa = -\Phi$, where κ and Φ are angles of rotation from the molecular x axis. The Φ and κ values calculated for (A) *Pa* cyt c_{551} and (B) horse cyt *c* assuming Φ is the mean angle of the two ligands are shown, using $\kappa = -\Phi$. Calculated values of κ are in general agreement with experimental values.[6,87] The axial His orientation is shown with a red line, and the axial Met with a blue line. The bisector of these angles, the think purple line, defines Φ. The κ value predicted on the basis of this mean ligand angle is indicated with a thick green line. Note that the value of κ determined for *Ht* cyt c_{552}, −47°, is approximately the average of the values in A and B, consistent with the axial Met sampling the conformations in A and B.[6]

Walker has shown that heme methyl shift patterns in low-spin ferriheme proteins, which are dominated by the contact shift, can be related to heme axial ligand orientations via simple Hückel calculations.[16] Heme methyl shifts thus can be used as constraints for determining heme ligand geometries in protein structures.[17] Pseudocontact shifts are related to the heme axial ligand orientations via the "counterrotation rule". In this formalism, if the mean axial ligand plane is oriented at an angle Φ from a N−Fe−N axis in the heme plane, then the direction of the minimum χ value (χ_{xx}) is at an angle $\kappa = -\Phi$ from that same axis (Figure 4).[11,18,19] Pseudocontact shifts are now widely used for refining solution structures of paramagnetic proteins.[20]

In early studies, it was noted that cyt's *c* from different structural families tend to display different heme methyl shift patterns. Wüthrich reported that eukaryotic cyt's *c* typically exhibit a pairwise ordering of heme methyl resonances with methyls 8 and 3 downfield (at ∼30−35 ppm) of methyls 5 and 1 (at ∼10 ppm). In contrast, bacterial cyt's *c* structurally similar to *Pseudomonas aeruginosa* (*Pa*) cyt c_{551} (formally classified cyt's c_8)[8] usually display a reversed pattern, with methyls 5 and 1 appearing downfield of methyls 8 and 3 (Figure 3A,B).[21] These different patterns result from different orientations of the heme axial Met (the axial His tends to be aligned along the α,γ-meso axis in cyt's *c*). The Met

(13) McConnell, H. M.; Robertson, R. E. *J. Chem. Phys.* **1958**, *29*, 1361−1365.
(14) (a) Kurland, R. J.; McGarvey, B. R. *J. Magn. Reson.* **1970**, *2*, 286−301. (b) Bertini, I.; Luchinat, C. *Coord. Chem. Rev.* **1996**, *150*, 29−75.
(15) Walker, F. A. *Inorg. Chem.* **2003**, *42*, 4526−4544.
(16) Shokhirev, N. V.; Walker, F. A. *J. Biol. Inorg. Chem.* **1998**, *3*, 581−594.
(17) Banci, L.; Bertini, I.; Cavallaro, G.; Luchinat, C. *J. Biol. Inorg. Chem.* **2002**, *7*, 416−426.
(18) Turner, D. L. *Eur. J. Biochem.* **1995**, *227*, 829−837.
(19) Shokhirev, N. V.; Walker, F. A. *J. Am. Chem. Soc.* **1998**, *120*, 981−990.
(20) (a) Gochin, M.; Roder, H. *Protein Sci.* **1995**, *4*, 296−305. (b) Banci, L.; Bertini, I.; Bren, K. L.; Cremonini, M. A.; Gray, H. B.; Luchinat, C.; Turano, P. *J. Biol. Inorg. Chem.* **1996**, *1*, 117−126. (c) Banci, L.; Presenti, C. *J. Biol. Inorg. Chem.* **2000**, *5*, 422−431.

orientation seen for bacterial cyt's c_8 (Figure 1A) and eukaryotic cyt's *c* (Figure 1B) differ essentially by inversion through the axial Met sulfur. This change in ligand conformation results in a change in the Met ligand angle of ~56°.[6,16,22] The result is a striking change in the unpaired electron delocalization pattern on the heme macrocycle, reflected in the heme methyl shift pattern, as well as a change in the orientation of the magnetic axes (Figure 4), which is reflected in the pseudocontact shifts.[16,21,23]

Despite the advances made in relating hyperfine shifts to the details of heme−ligand interactions in cyt's *c*, some cyt's *c* display NMR properties that cannot be readily understood in this framework. The inability to explain hyperfine shifts in these proteins brought to question whether models relating heme ligation to electronic structure, and thus NMR spectra, are incomplete, or whether there were aspects of heme−ligand interactions not understood in some proteins.[16,24,25] In particular, cyt's c_{552} from *Ne*[16,24] and from *Hydrogenobacter thermophilus* (*Ht*)[6,25] were reported to exhibit anomalous, highly compressed heme methyl shift patterns, not readily interpreted in terms of a single orientation of the His and Met axial ligands (Figure 3). NMR studies of these proteins, discussed below, have advanced our understanding of heme ligation properties in proteins.

These developments in our understanding of the factors that determine chemical shifts in paramagnetic heme proteins have made NMR spectroscopy an important tool for investigating structure, folding, and dynamics of ferricyt's *c*. Another vital advance aiding the use of NMR spectroscopy to probe cyt *c* folding and dynamics has been the development of expression systems capable of producing wild-type and mutated correctly folded holocyt's *c* in high yield.[26,27] Correct covalent attachment of heme to the cytochrome polypeptide is a necessary step for achieving the native cyt *c* fold. Study of this process led to development of highly effective expression systems for a range of cyt's *c*.

In Vivo Cytochrome *c* Assembly and Folding

The synthesis and folding of functional proteins within the cell requires the assistance of chaperones and proteins that perform posttranslational modifications and quality control.[28] In the case of cyt's *c*, covalent heme attachment to the polypeptide is a posttranslational event required to achieve native stability and folding and is assisted by the products of cyt *c* maturation genes (in *Escherichia coli*, *ccmABCDEFGH*).[29,30] Successful heterologous overexpression of cyt's *c* thus requires overexpression both of a cyt *c* structural gene and genes encoding factors that assist with heme attachment.[26,27] Prior to the development of expression/maturation systems producing correctly folded holocyt's *c*, however, expression of thermophilic holocyt's c_{552} from *Ht*[31] and from *Thermus thermophilus* (*Tt*)[32] in *E. coli* was reported. Interestingly, holoprotein formed spontaneously without assistance of ccm factors in both cases.[33] These results raised the general question of why nature employs a complex cyt *c* maturation process. It was found, however, that whereas the *Ht* holocyt c_{552} formed correctly without assistance in the *E. coli* cytoplasm,[25,33] the products of expression of the *Tt* cyt c_{552} gene exhibited errors.[34] The study of these products of incorrect recombinant *Tt* cyt c_{552} maturation by Fee and co-workers provided insights into in vivo assembly and folding of cyt's *c*. This work also illustrates the important role NMR spectroscopy can play in characterizing both subtle and significant perturbations to folding and electronic structure in expression products.

One product of *Tt* cyt c_{552} expression, *Tt* rC_{552}, was monomeric and displayed properties generally similar to those of the authentic protein (i.e., protein from *Tt* cells).[32] Close study, however, revealed structural and spectroscopic differences between rC_{552} and authentic protein. The 1.41-Å crystal structure of rC_{552} revealed an overall nativelike fold, but with differences around heme ring I in rC_{552} compared to authentic *Tt* cyt c_{552}. The structure reveals an abnormal thioether linkage between Cys11 (the first in the Cys−X−X−Cys−His motif) and the heme 2-vinyl, consistent with a $-CO-CH_2-S-CH_2-$ linkage (Figure 5A).[35] NMR studies of the rC_{552} solution conformation were consistent with this finding; the hyperfine-shifted resonances for ferric rC_{552} differed (although not radically) from those observed for authentic protein, indicating perturbation of the heme and/or its environment (Figure 6A,C).[32,35] This is consistent with the linkage observed in the X-ray structure in which the linkage carbonyl is not coplanar with the porphyrin. Importantly, NMR data also revealed that rC_{552} was partially unfolded in solution,[35] consistent with the proposal that the

(21) Senn, H.; Wüthrich, K. *Q. Rev. Biophys.* **1985**, *18*, 111−134.
(22) For Met, the orientation angle is determined by projecting the bisector of the Met Cγ−Sδ−Cε angle onto the heme plane and taking a vector perpendicular to this projection. The orientation angle of Met is the angle between this vector and the heme *x* axis. For His, the orientation angle is the angle between the ligand imidazole plane and the *xz* plane of the molecular coordinate system.
(23) Santos, H.; Turner, D. L. *Magn. Reson. Chem.* **1993**, *31*, s90−s95.
(24) Timkovich, R.; Cai, M.; Zhang, B.; Arciero, D. M.; Hooper, A. B. *Eur. J. Biochem.* **1994**, *226*, 159−168.
(25) Karan, E. F.; Russell, B. S.; Bren, K. L. *J. Biol. Inorg. Chem.* **2002**, *7*, 260−272.
(26) Arslan, E.; Schulz, H.; Zufferey, R.; Künzler, P.; Thöny-Meyer, L. *Biochem. Biophys. Res. Commun.* **1998**, *251*, 744−747.
(27) Pollock, W. B. R.; Rosell, F. I.; Twitchett, M. B.; Dumont, M. E.; Mauk, A. G. *Biochemistry* **1998**, *37*, 6124−6131.
(28) Feldman, D. E.; Frydman, J. *Curr. Opin. Struct. Biol.* **2000**, *10*, 26−33. (b) Tsunasawa, S.; Stewart, J. W.; Sherman, F. *J. Biol. Chem.* **1985**, *260*, 5382−5391. (c) Wickner, S.; Maurizi, M. R.; Gottesman, S. *Science* **1999**, *286*, 1888−1893.
(29) Kranz, R.; Lill, R.; Goldman, B.; Bonnard, G.; Merchant, S. *Mol. Microbiol.* **1998**, *89*, 383−396.
(30) Tomlinson, E. J.; Ferguson, S. J. *Proc. Natl. Acad. Sci. U.S.A.* **2000**, *97*, 5156−5160.
(31) Sanbongi, Y.; Yang, J.-H.; Igarashi, Y.; Kodama, T. *Eur. J. Biochem.* **1991**, *198*, 7−12.
(32) Keightley, J. A.; Sanders, D.; Todaro, T. R.; Pastuszyn, A.; Fee, J. A. *J. Biol. Chem.* **1998**, *273*, 12006−12016.
(33) Sambongi, Y.; Crooke, H.; Cole, J. A.; Ferguson, S. J. *FEBS Lett.* **1994**, *344*, 207−210.
(34) Fee, J. A.; Chen, Y.; Todaro, T. R.; Bren, K. L.; Patel, K. M.; Hill, M. G.; Gomez-Moran, E.; Loehr, T. M.; Ai, J.; Thöny-Meyer, L.; Williams, P. A.; Stura, E.; Sridhar, V.; McRee, D. E. *Protein Sci.* **2000**, *9*, 2074−2084.
(35) Fee, J. A.; Todaro, T. R.; Luna, E.; Sanders, D.; Hunsicker-Wang, L.; Patel, K. M.; Bren, K. L.; Gomez-Moran, E.; Hill, M. G.; Ai, J.; Loehr, T. M.; Oertling, W. A.; Williams, P. A.; Stout, C. D.; McRee, D.; Pastuszyn, A. *Biochemistry* **2004**, *43*, 12162−12176.

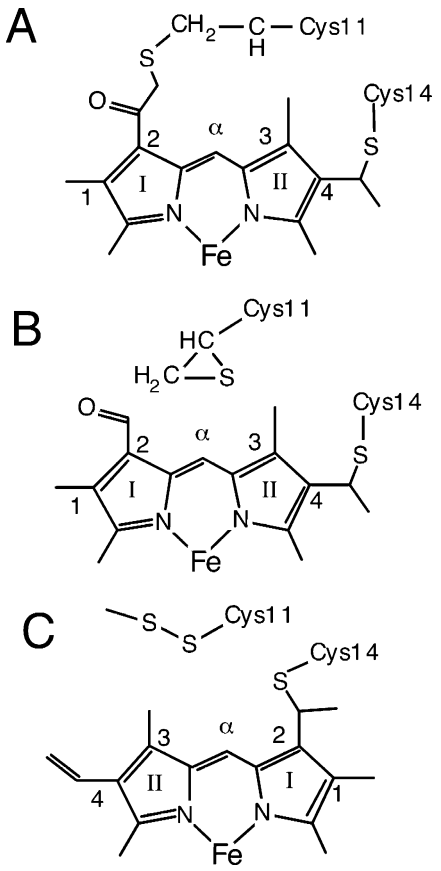

Figure 5. Results of anomalous *Tt* cyt c_{552} maturation on heme structure. Shown are proposed heme structures for (A) *Tt* rC_{552}, (B) *Tt* p572, and (C) *Tt* rC_{557}. The particularly large differences in the NMR and absorption spectra of rC_{552} and p572 result from the carbonyl group being in the plane of the heme in B, but not in A. Note the altered orientation of the heme in C relative to A and B.

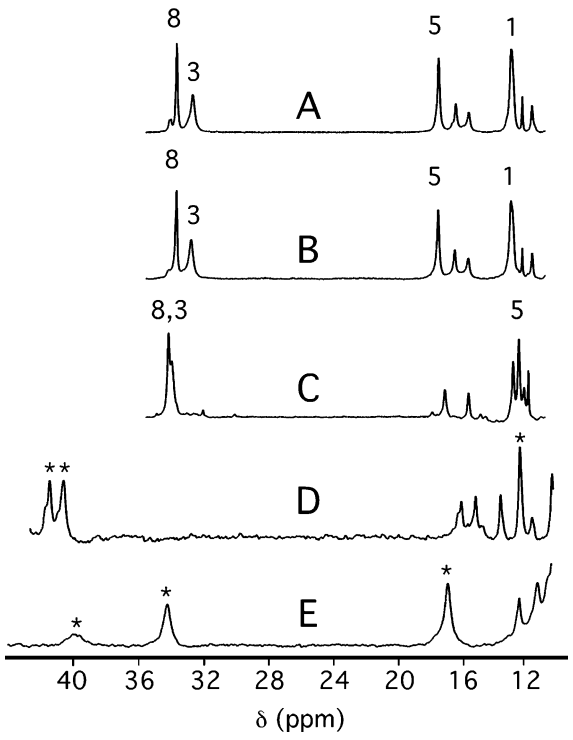

Figure 6. 500-MHz NMR spectra (100 mM NaP_i, 90% D_2O/10% H_2O, pH 7.0, 25 °C) of *T. thermophilus* cytochromes c_{552}. Shown are downfield regions of spectra of (A) authentic *Tt* cyt c_{552},[34] (B) recombinant *Tt* cyt c_{552} that underwent maturation via the normal bacterial pathway (*Tt* rsC_{552}),[34,35] (C) incorrectly matured recombinant *Tt* cyt c_{552} from the *E. coli* cytoplasm (*Tt* rC_{552}),[34] (D) *Tt* p572,[38] and (E) *Tt* rC_{557}.[35] Heme methyl assignments, when known, are indicated. Asterisks (*) indicate resonances attributed to heme methyls but not assigned to specific heme methyls. These data demonstrate that heme attachment did not proceed correctly by the spontaneous route, but when directed to utilize the enzymatic route, gave a nativelike protein.

incorrectly matured protein exists as a "molten globule".[36] Thus, NMR spectroscopy revealed that the incorrect heme−protein linkage in rC_{552} caused by anomalous maturation is associated both with minor perturbation of heme electronic structure and with a significant compromise of protein fold integrity.

Another product of *Tt* cyt c_{552} gene expression, *Tt* p572, could be formed by gentle heating or denaturation of rC_{552}. Despite the unusual green color and α-band at 572 nm, His-Met heme ligation was confirmed in both oxidation states of p572. The crystal structure of p572 reveals a modified heme, consistent with a formyl group coplanar with the porphyrin at position 2 (Figure 5B). The heme axial ligands, however, bind heme iron in conformations similar those seen in rC_{552} and in authentic protein.[35] Significant changes in the NMR spectrum of p572 relative to rC_{552} were observed, with the appearance of resonances with unusually high shifts for low-spin heme (two resonances at >40 ppm at 25 °C; Figure 6D). It previously has been shown that perturbation of heme structure by addition of peripheral acetyl or formyl groups leads to strong perturbation of heme hyperfine shifts.[37] In p572, the presence of an electron-withdrawing formyl group at position 2 would induce a strong rhombic electronic perturbation along the pyrrole I, III vector, which in turn is expected to lead to increased hyperfine shifts for substituents on pyrroles II and IV. The unusually high values of the heme methyl shifts measured for p572 along with their large spread can be explained by the combination of the effects of nativelike heme−ligand interactions and the presence of the formyl group at position 2, because each of these effects directs unpaired electron spin density to pyrroles II and IV. The ^{1}H NMR spectrum of oxidized p572 thus is consistent with the presence of an electron-withdrawing group on pyrrole I.[35] As for rC_{552}, NMR spectroscopy indicated that p572 existed in a partially folded state in solution.

A third expression product was the dimeric *Tt* rC_{557}, also with His-Met heme ligation. Substantial differences were detected between the pattern of hyperfine-shifted resonances for rC_{557} and those for authentic protein, indicating dimerization was accompanied by a perturbation of the heme site (Figure 6E). The crystal structure (Figure 7) revealed a heme incorrectly incorporated into the cytochrome polypeptide, with a rotation about the α,γ-meso axis (Figure 5C).[38] The heme in rC_{557} is attached to only a single Cys, which

(36) Wittung-Stafshede, P. *Biochim. Biophys. Acta* **1998**, *1362*, 324−332.
(37) La Mar, G. N.; Budd, D. L.; Viscio, D. B.; Smith, K. M.; Langry, K. C. *Proc. Natl. Acad. Sci.* **1978**, *75*, 5755−5759.
(38) McRee, D. E.; Williams, P. A.; Sridhar, V.; Pastuszyn, A.; Bren, K. L.; Patel, K. M.; Chen, Y.; Todaro, T. R.; Sanders, D.; Luna, E.; Fee, J. A. *J. Biol. Chem.* **2001**, *276*, 6537−6544.

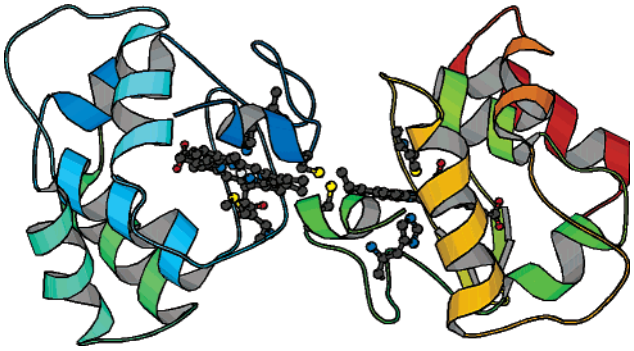

Figure 7. X-ray crystal structure of *Tt* rC_{557} (PDB identifier 1FOC). Note that the two Cys moieties (from the Cys−X−X−Cys−His motif) at the dimer interface form a disulfide link.

accounts for the 5-nm red shift of the low-energy absorption band in the ferrous protein; the other Cys forms a disulfide link across the dimer interface. The NMR properties confirmed a substantial perturbation of the heme environment and are consistent with a heme reorientation relative to authentic protein.[38] The NMR results suggest that the formation of the rC_{557} dimer requires misorientation of the heme, as resonances similar to those seen for authentic protein or for rC_{552} were not observed.

Studies of the results of anomalous maturation of *Tt* cyt c_{552} thus revealed three misfolded products of improper cyt *c* maturation with heme attachment errors. These data suggest that maturation factors assist in obtaining the correct heme orientation within the protein and are needed to direct the Cys thiol to attack the correct (Cα) heme vinyl carbon. A surprising consequence of attachment to the incorrect vinyl carbon (Cβ) was formation of a product (rC_{552}) that could react further to yield a 2-formyl heme, resulting in p572.[35] Errors in heme attachment also were shown by NMR spectroscopy to cause significant perturbation of the integrity of the protein fold in solution.[34,35,38] These maturation errors were corrected by directing the *Tt* cyt c_{552} polypeptide upon expression to the *E. coli* periplasm by incorporation of a translocation sequence, and overexpressing the *ccm* genes, allowing for maturation along the "normal" bacterial pathway, yielding properly folded holoprotein (rsC_{552}; Figure 6B).[34]

NMR Investigations of Cytochrome *c* Denatured States

In recent years, general interest in the properties of unfolded, partially folded, and misfolded proteins has increased because of the recognition of their importance in phenomena including determination of protein stability and protein-mediated diseases.[39,40] In the field of protein folding, it is recognized that characterization of unfolded and partially unfolded proteins aids in gaining an understanding of how proteins acquire their native structure.[39] NMR spectroscopy is well-suited for the characterization of disordered forms of proteins because it allows detailed studies to be carried

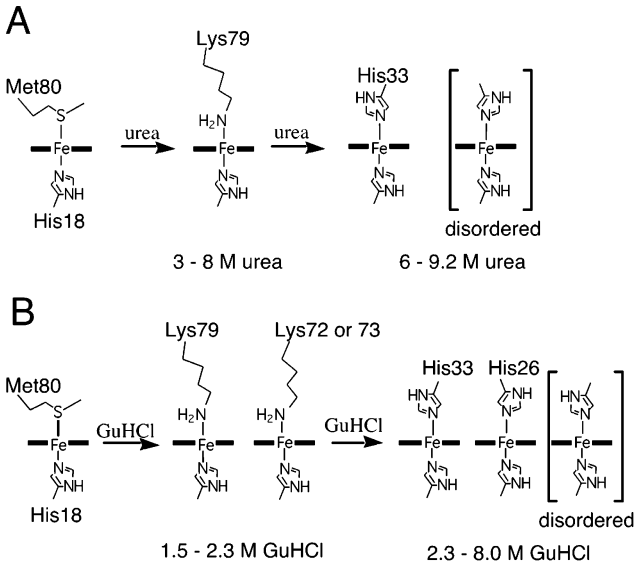

Figure 8. Summary of nonnative heme ligation for horse ferricyt *c* in urea and GuHCl detected by NMR spectroscopy. (A) In urea, one intermediate with His-Lys heme ligation and one denatured form with bis-His heme ligation are detected. It is proposed that the nonnative Lys is Lys79 and that the nonnative His is His33. (B) In GuHCl, two intermediates with His-Lys heme ligation and two denatured forms with bis-His heme ligation are detected. In both cases, it is likely that additional, more highly disordered forms with bis-His heme ligation also are present but cannot be detected by analysis of heme methyl shifts.[4,5]

out through a range of solvent conditions. NMR spectroscopy of disordered proteins, however, presents substantial challenges because unfolded and partially unfolded proteins display substantial conformational exchange as well as low chemical shift dispersion, particularly for proton shifts, which are especially important for structure determination.[41]

As chemical shift dispersion is inherently higher in paramagnetic than in diamagnetic molecules, proteins that bind paramagnetic metals in the denatured state make attractive subjects of NMR studies. For example, as illustrated in the previous section, NMR studies facilitated the characterization of cyt's *c* with maturation and folding errors. NMR spectroscopy is a useful tool also for the study of protein denaturation. Mitochondrial cyt's *c* have long been known to undergo heme ligand exchange upon unfolding, with the native Met80 axial ligand being replaced by one or more strong-field ligands (His in the unfolded state) while the native His18 remains in place (Figure 8).[10,42] The coupling between cyt *c* unfolding and heme ligand switching provides an excellent handle by which to characterize denatured paramagnetic cyt *c* by NMR spectroscopy. This approach takes advantage of the high sensitivity of the heme substituent shifts to the type and orientation of heme axial ligands.

For horse ferricyt *c*, it was reported that well-resolved hyperfine-shifted resonances could be detected and assigned even under strongly denaturing conditions.[4,5] Studies of ferricyt *c* unfolding in urea led to elucidation of heme axial ligation in nonnative forms. Resonance assignments and use of chemically modified derivatives revealed the denatured

(39) (a) Shortle, D. *Curr. Opin. Struct. Biol.* **1993**, *3*, 66−74. (b) Shortle, D. *FASEB J.* **1996**, *10*, 27−34.
(40) (a) Thomas, P. J.; Qu, B. H.; Pedersen, P. L. *Trends Biochem. Sci.* **1995**, *20*, 456−459. (b) Radford, S. E.; Dobson, C. M. *Cell* **1999**, *97*, 291−298.
(41) Yao, J.; Dyson, H. J.; Wright, P. E. *FEBS Lett.* **1997**, *419*, 285−289.
(42) Muthukrishnan, K.; Nall, B. T. *Biochemistry* **1991,** *30*, 4706−4710.

form observed in urea to have His18/His33 heme ligation, where His33 surprisingly samples a relatively small range of angles relative to the heme axes.[4,5] Interestingly, upon guanidinium hydrochloride (GuHCl) denaturation, both His18/His33 and His18/His26 forms were observed by NMR spectroscopy, indicating a difference in the denatured state depending on the type of denaturant used.[5] Kinetics analysis of the folding of cyt *c* mutants in the Roder lab, however, indicated that His33 binding influences folding kinetics in GuHCl whereas His26 binding does not.[43] These studies have important implications for protein folding studies that employ denaturants.

Another surprising result of NMR studies of horse ferricyt *c* unfolding was the finding that a compact folding intermediate with His/Lys heme axial ligation was populated at intermediate urea concentrations at neutral pH.[4] Unlike the alkaline conformers of cyt *c*, of which there are two (attributed to ligation of Lys79 and Lys73 in *S. cerevisiae* iso-1-ferricyt *c*; more than two can exist in horse ferricyt *c*),[44] only one conformer with His/Lys ligation was detected for horse ferricyt *c* in urea.[4] In the presence of GuHCl, however, two forms attributed to His/Lys ligation were detected.[5] Thus, the properties of folding intermediates also depend on the denaturant used. These results point out the ever-present possibility of the existence of "hidden" intermediates in protein folding; the ability to detect an intermediate depends on the probe used.[45] Here, it is the presence of a paramagnetic heme that allowed NMR detection of these intermediates. Notably, His/Lys ligation has been proposed for kinetic cyt *c* folding intermediates, suggesting that the forms observed at equilibrium might have relevance for the kinetic folding pathway.[46]

NMR Investigations of Cytochrome *c* Backbone Dynamics

Characterizing folded-state dynamics of proteins is vital for making meaningful links between structure and function.[47] Currently, our general understanding of how the protein fold is related to protein dynamical properties, and how dynamics relate to function, is limited. It is understood, however, that protein dynamics play a vital role for modulating function, even when that function is as seemingly simple as electron transfer.[48−50] In metalloproteins, dynamics of overall protein structure as well as the immediate environment of the metal active site can influence electron-transfer rates and interactions with redox partners. The necessary step of characterizing protein dynamics is a demanding task because of the large range of time and length scales over which protein dynamics occur. Nevertheless, progress has been made by employing a variety of techniques, and NMR spectroscopy has proven particularly valuable for providing detailed, site-specific information on dynamics on time scales from picoseconds to seconds. For the protein backbone, this information is obtained through measurement and analysis of relaxation properties of ^{15}N nuclei, and of hydrogen exchange rates, which are determined by local and global mobility.[51]

The development of *E. coli*-based expression systems for cyt's *c* made it feasible to produce isotopically labeled cyt's *c* in amounts needed for nuclear relaxation studies. The cyt *c* family, having a large number of members with varying degrees of homology, is an attractive target for general studies of the structure−dynamics relationship. For example, despite low sequence homology, the overall topologies of bacterial (cyt c_8 classification as a specific example here) and mitochondrial class I cyt's *c* are generally similar (Figure 2A−C).

Because many cyt's *c* share a similar fold, the same function of electron transfer, and a low-spin *c*-type heme, it might be expected that proteins in this family would display generally similar dynamics. Analysis of backbone dynamics now has been performed on a number of bacterial and photosynthetic *c*-type cytochromes, and also on mitochondrial cyt *c* from *S. cerevisiae* (for examples, see refs 52−62). Indeed, for most cyt's *c*, the structures generally have high and uniform rigidity (Figure 9). *S. cerevisiae* iso-1-ferricyt *c*, however, diverges from this trend. In particular, loop 3, containing the axial Met (Figure 2), displays enhanced dynamics in *S. cerevisiae* iso-1-ferricyt *c* according to measures sensitive to short time scale (picoseconds to nanoseconds) motions relative to smaller bacterial cyt's *c*.[56−58] This loop also experiences low-energy local fluctuations in horse and in *S. cerevisiae* iso-1-ferricyt's *c* as revealed by hydrogen exchange studies[59,60] and by nuclear relaxation studies sensitive to microsecond time scale mo-

(43) Colón, W.; Wakem, L. P.; Sherman, F.; Roder, H. *Biochemistry* **1997**, *36*, 12535−12541.
(44) (a) Hong, X.; Dixon, D. W. *FEBS Lett.* **1989**, *246*, 105−108. (b) Rosell, F. I.; Ferrer, J. C.; Mauk, A. G. *J. Am. Chem. Soc.* **1998**, *120*, 11234−11245.
(45) Zeeb, M.; Rosner, H.; Zeslawski, W.; Canet, D.; Holak, T. A.; Balbach. J. *J. Mol. Biol.* **2002**, *315*, 447−457.
(46) Tezcan, F. A.; Winkler, J. R.; Gray, H. B. *J. Am. Chem. Soc.* **1999**, *121*, 11918−11919.
(47) (a) Cheung, M. S,.; Chavez, L. L.; Onuchic, J. N. *Polymer* **2004**, *45*, 547−555. (b) Daniel, R. M.; Dunn, R. V.; Finney, J. L.; Smith, J. C. *Annu. Rev. Biophys. Biomol. Struct.* **2003**, *32*, 69−92.
(48) Ehrenberg, A. *Biochim. Biophys. Acta* **2004**, *1665*, 231−234.
(49) Marcus, R. A.; Sutin, N. *Biochim. Biophys. Acta* **1985**, *811*, 265−322.
(50) Daizadeh, I.; Medvedev, E. S.; Stuchebrukhov, A. A. *Proc. Natl. Acad. Sci. U.S.A.* **1997**, *94*, 3703−3708.
(51) Ishima, R.; Torchia, D. A. *Nature Struct. Biol.* **2000**, *7*, 740−743.
(52) Ubbink, M.; Pfuhl, M.; Van der Oost, J.; Berg, A.; Canters, G. W. *Protein Sci.* **1996**, *5*, 2494−2505.
(53) Flynn, P. F.; Urbauer, R. J. B.; Zhang, H.; Lee, A. L.; Wand, A. J. *Biochemistry* **2001**, *40*, 6559−6569.
(54) Cordier, F.; Caffrey, M.; Brutscher, B.; Cusanovich, M. A.; Marion, D.; Blackledge, M. *J. Mol. Biol.* **1998**, *281*, 341−361.
(55) Reincke, B.; Pérez, C.; Pristovsek, P.; Lücke, C.; Ludwig, C.; Löhr, F.; Rogov, V. V.; Ludwig, B.; Rüterjans, H. *Biochemistry* **2001**, *40*, 12312−12320.
(56) Fetrow, J. S.; Baxter, S. M. *Biochemistry* **1999**, *38*, 4480−4492.
(57) Russell, B. S.; Zhong, L.; Bigotti, M. G.; Cutruzzolà, F.; Bren, K. L. *J. Biol. Inorg. Chem.* **2003**, *8*, 156−166.
(58) Banci, L.; Bertini, I.; Ciurli, S.; Dikiy, A.; Dittmer, J.; Rosato, A.; Sciara, G.; Thompsett, A. R. *ChemBioChem* **2002**, *3*, 299−310.
(59) Bai, Y. W.; Sosnick, T. R.; Mayne, L.; Englander, S. W. *Science* **1995**, *269*, 192−197.
(60) Baxter, S. M.; Fetrow, J. S. *Biochemistry* **1999**, *38*, 4493−4503.
(61) Barker, P. D.; Bertini, I.; Del Conte, R.; Ferguson, S. J.; Hajieva, P.; Tomlinson, E.; Turano, P.; Vieszzoli, M. S. *Eur. J. Biochem.* **2001**, *268*, 4468−4476
(62) Bartalesi, I.; Bertini, I.; Ghosh, K.; Rosato, A.; Turano, P. *J. Mol. Biol.* **2002**, *321*, 693−701.

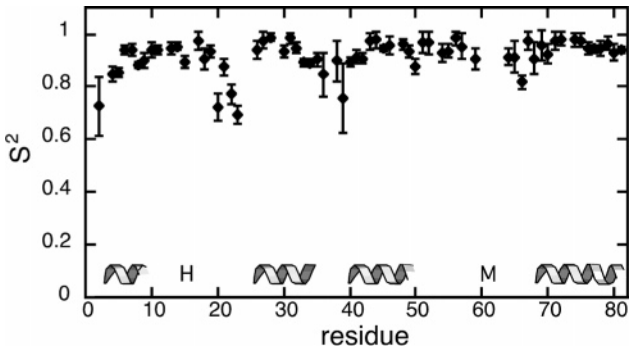

Figure 9. Results of model-free analysis of ^{15}N relaxation properties of backbone nuclei in *Pa* ferricyt c_{551}. Helical regions are indicated, and H and M mark the axial ligand positions. Values for order parameters (S^2) that describe the magnitude of angular motions of backbone NH bond vectors on the picosecond to nanosecond time scale are plotted against sequence. Order parameters range from 0 (isotropic motion) to 1 (rigid). Note the high and uniform nature of the S^2 values and the high values in the 50−67 loop region (the Met-bearing loop). From ref 57.

tion.[61] The structural basis for the pronounced dynamics in the mitochondrial cyt *c* Met-donating loop is not clear, although a lack of long-range hydrogen bonds and other interactions involving this loop in the mitochondrial proteins has been noted.[57,62] Differences in amino acid composition[57,62] and length[62] of loop 3 also have been proposed to contribute to differences in dynamics of this loop seen in the mitochondrial vs the small bacterial cyt's *c*. It also is possible that the flexibility of loop 3 in mitochondrial cyt *c* is related to its sampling of a low-energy unfolding intermediate.[4,57,59,62]

Also of interest are the functional consequences of the different properties of the Met-donating loop in these cytochromes. Analysis of high-resolution crystal structures in both oxidation states reveals a larger change in Fe−S bond length upon oxidation of y-cyt *c* (∼0.1 Å)[63] relative to *Pa* cyt c_{551} (∼0.01 Å).[6,64] The flexibility of loop 3 in the mitochondrial proteins might be what allows a greater structural rearrangement in response to change in iron redox state,[6] although this hypothesis awaits an experimental test. These differences also could have implications for determination of inner-sphere reorganization energies of these proteins.[49] The evolutionary advantage to mitochondrial cyt *c* in having a flexible loop 3 is not clear, although the mobility of the Met-containing domain in mitochondrial cyt's *c* is proposed to modulate binding to redox partners.[65] It also has been proposed that conformational rearrangements of cyt *c* might occur during apoptosis, a function displayed specifically by mitochondrial cyt *c*.[66]

Protein Dynamics and Heme Electronic Structure

The Met−Fe interaction in cyt's *c* plays an important role in determining heme electronic structure. The thioether−Fe(III) interaction is inherently weak,[67] and indeed, it has been proposed that the thioether heme−protein linkages are required to enhance the effective ligand field strength of Met to yield a low-spin heme.[68] The specific properties of the protein fold are expected to play an important role in modulating the Met−Fe interaction.[6,57,62] Different axial Met orientations thus are observed within different cyt *c* folds, although the details of how the fold determines Met orientation and whether there exist functional consequences of Met orientation differences remain open questions.[21,24]

In most cases, the relationship between cyt *c* axial Met orientation and heme methyl shifts is relatively clear: proteins with Met orientation shown in Figure 1A (for example, *Pa* cyt c_{551}) have the 5-CH_3 > 1-CH_3 > 8-CH_3 > 3-CH_3 pattern (Figure 3A), and proteins with Met orientation shown in Figure 1B (for example, horse cyt *c*) show the reverse pairwise pattern (8-CH_3 > 3-CH_3 > 5-CH_3 > 1-CH_3; Figure 3B). There are two bacterial (cyt c_8) cytochromes, however, with heme methyl shift patterns seemingly not consistent with any combination of axial ligand orientations, cyt's c_{552} from *Ne*[24] and *Ht*.[25] Both have similar shifts for all four heme methyl groups, indicating a more axial electronic structure than is typical for cyt's *c* (Figure 3C,D). The relatively axial character of these cytochromes also is revealed by the low magnitude rhombic anisotropy for *Ht* cyt c_{552} determined by analysis of pseudocontact shifts.[6] It also is notable that *Ne* cyt c_{552} displays an axial EPR signal.[69]

In the case of *Ht* cyt c_{552}, the puzzle of the compressed heme methyl shift range recently was addressed by raising the possibility that heme axial ligands in proteins might display substantial conformational dynamics, as is commonly observed in transition metal complexes.[6] Cyt's *c* are generally assumed to have a well-defined axial Met (and His) orientation; the two most common Met orientations are shown in Figure 1.[70] If, however, the heme axial Met in *Ht* cyt c_{552} were to sample both of these conformations rapidly on the NMR time scale, a spectrum resulting from averaging of the shifts expected in the two limiting conformations would result (Figure 3). In addition, one would expect the magnetic axes to be oriented in an "average" position, as is observed (Figure 4). Confirmation that motional averaging affecting the heme methyl shifts is occurring was obtained by observing line broadening of the *Ht* cyt c_{552} heme methyls independent of T_1 as temperature is lowered. Successful simulation of the broad lines observed, based on expected shifts in the extreme conformations provides additional support for this theory.[6]

The cause of this unusual heme ligand fluxionality has been proposed to be the high rigidity of the Met-donating

(63) Berghuis, A. M.; Brayer, G. D. *J. Mol. Biol.* **1992**, *223*, 959−976.
(64) Matsuura, Y.; Takano, T.; Dickerson, R. E. *J. Mol. Biol.* **1982**, *156*, 389−409.
(65) Berghuis, A. M.; Guillemette, J. G.; McLendon, G.; Sherman, F.; Smith, M.; Brayer, G. D. *J. Mol. Biol.* **1994**, *236*, 786−799.
(66) (a) Jemmerson, R.; Liu, J.; Hausauer, D.; Lam, K. P.; Mondino, A.; Nelson, R. D. *Biochemistry* **1999**, *38*, 3599−3609. (b) Chevance, S.; Le Rumeur, E.; de Certaines, J. D.; Simonneaux, G.; Bondon, A. *Biochemistry* **2003**, *42*, 15342−15351.
(67) (a) Murray, S. G.; Hartley, F. R. *Chem. Rev.* **1981**, *81*, 365−414. (b) Smith, M.; McLendon, G. *J. Am. Chem. Soc.* **1981**, *103*, 4912−4921. (c) Tezcan, F. A.; Winkler, J. R.; Gray, H. B. *J. Am. Chem. Soc.* **1998**, *120*, 13383−13388.
(68) Cowley, A. B.; Lukat-Rodgers, G. S.; Rodgers, K.R.; Benson, D. R. *Biochemistry* **2004**, *43*, 1656−1666.
(69) Arciero, D. M.; Peng, Q. Y.; Peterson, J.; Hooper, A. B. *FEBS Lett.* **1994**, *342*, 217−220.
(70) The orientation of the axial His is similar across cyt's *c* and likely is determined by local constraints imposed by the Cys-heme covalent bonds as well as the His-Fe bond. Thus, significant motion of the axial His is not likely. Low, D. W.; Gray, H. B.; Duus, J. Ø. *J. Am. Chem. Soc.* **1997**, *119*, 1−5.

loop in the cyt c_8 family, combined with the possibility of either steric crowding or the lack of a hydrogen bond to the axial Met sulfur in the heme pocket of *Ht* cyt c_{552}.[6] Notably, another member of the cyt c_8 family, *Ne* cyt c_{552}, displays an unusually compressed heme methyl shift range.[24] To date, a satisfactory explanation of the *Ne* ferricyt c_{552} shift pattern has not appeared.[16] We propose here that, as in *Ht* cyt c_{552}, a dynamical process involving the axial Met is occurring in *Ne* cyt c_{552} to yield an unusually compressed heme methyl shift range. Indeed, this protein is structurally highly homologous to *Ht* cyt c_{552}.[71,72] Like *Ht* cyt c_{552}, *Ne* cyt c_{552} displays anomalies in the structure of the Met-donating loop that set it apart from other members of the cyt c_8 family. In particular, there is a one-residue insertion in the Met-donating loop in *Ne* cyt c_{552} that causes the loop to pack differently against the heme in comparison with other proteins in this family (*Pa* cyt c_{551} being the prototypical member).[72] To address this interesting question, we employ here the cyt *c* expression system described above[25,34] to express *Ne* cyt c_{552}. We performed variable-temperature NMR studies and T_1 measurements on *Ne* ferricyt c_{552} to show that the NMR properties of this protein are consistent with axial ligand dynamics.

Results

***Ne* Cyt c_{552} Expression and Initial Characterization.** Yields of highly purified recombinant wild-type *Ne* cyt c_{552} (NE hereafter) were ~5 mg/L. Fast protein liquid chromatography (FPLC) purification yielded a major peak eluting at 70 mM NaCl, followed by a substantial tailing of minor forms. The molecular mass of NE was determined to be 9096 ± 3 amu by MALDI-TOF mass spectrometry, which compares well with the expected value (based on the amino acid sequence) of 9098 amu. The absorption spectra of oxidized and reduced NE (Supporting Information) are typical of *c*-type cytochromes. The low-energy band in the spectrum of reduced NE is at 551 nm, as reported elsewhere,[72] and displays the subtle splitting often seen in cyt's *c*.[34,73] For the oxidized proteins, a weak absorption band is observed at 692 nm, indicative of Met−Fe(III) ligation.[7,8] The absorption spectrum of the pyridine hemochrome reveals α- and β-bands at 550 and 520 nm, respectively, consistent with a *c*-type heme.[74] The circular dichroism (CD) spectrum of NE has minima at 208 and 222 nm, consistent with a protein with α-helical content as expected (Supporting Information).

NMR Spectroscopy. The 1-D ^{1}H NMR spectrum of oxidized NE displays heme methyl proton shifts (1-CH_3, 3-CH_3, 5-CH_3, 8-CH_3) of 20.0, 22.5, 24.2, and 22.7 ppm, respectively, at 333 K (Figure 3D). These agree with the shifts for authentic *Ne* Fe(III)cyt c_{552} (20.2, 22.4, 24.4, and 22.7 ppm at 333 K).[24] The similarity between the shifts for the authentic and recombinant wild-type proteins indicates that the recombinant protein has a heme environment similar to that of authentic protein. In the NMR spectrum of reduced NE, the characteristic resonances of the axial Met that are shifted upfield by the ring current are detected (Supporting Information). The chemical shifts (ppm) measured for NE compare well to those reported for authentic protein (authentic in parentheses): axial Met ε-CH_3 −3.15 (−3.15), Hγ −3.70 (−3.73), Hβ −2.88 (−2.85).[72] This finding confirms axial Met ligation in the reduced form of NE and similarity of this ligation to authentic protein.

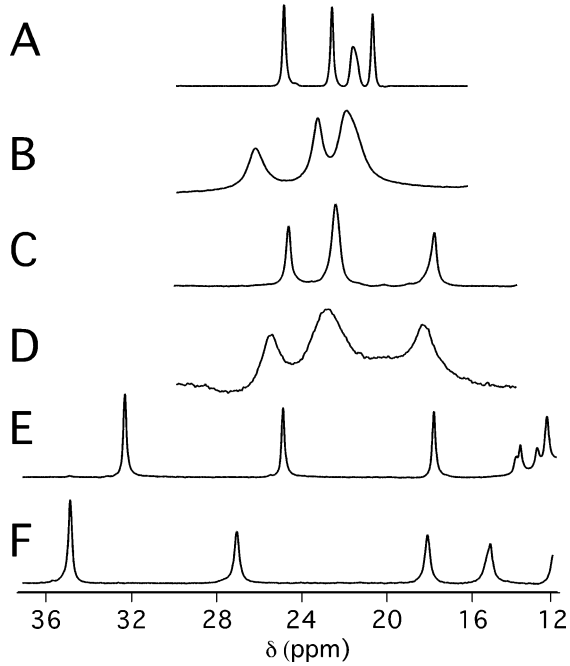

Figure 10. Downfield regions of variable-temperature 500-MHz ^{1}H NMR spectra used to analyze ferricyt *c* heme site dynamics. Samples are in 50 mM sodium phosphate buffer, pH 7.0, with 20% v/v CD_3OD and a 5-fold molar excess of $K_3Fe(CN)_6$ added. (A) *Ne* cyt c_{552}, 298 K; (B) *Ne* cyt c_{552}, 266 K; (C) *Ht* cyt c_{552}, 298 K; (D) *Ht* cyt c_{552}, 266 K; (E) *Pa* cyt c_{551}, 298 K; and (F) *Pa* cyt c_{551}, 266 K. The broadening seen at low temperature in B and D is proposed to result from chemical exchange. Significant broadening is not observed for the heme methyls of *Pa* cyt c_{551}.

Addition of CD_3OD (20% v/v) to NE samples leads to slight line broadening of the heme methyl peaks, in particular for the 3-CH_3 resonance (Figure 10A; compare to Figure 3D). The chemical shift dispersion and line widths throughout the NMR spectrum, however, indicate that the protein nevertheless maintains a nativelike fold. A similar line broadening effect upon addition of methanol has been observed for the heme methyls of *Ht* cyt c_{552}[6] and horse cyt *c*.[75] Lowering of the temperature to 266 K results in pronounced line broadening for NE (Figure 10B), similar to that seen for *Ht* ferricyt c_{552} (Figure 10C,D) and in contrast to the behavior of *Pa* ferricyt c_{551}, which shows little line broadening (Figure 10E,F).[6] Estimates of the respective T_1 values for the oxidized NE heme methyls (8-CH_3 and 5-CH_3) were 140 and 110 ms, respectively, at 298 K and 120 and 90 ms at 266 K (the peaks for 1-CH_3 and 3-CH_3 overlap at

(71) Hasegawa, J.; Yoshida, T.; Yamazaki , Y.; Sambongi, Y.; Yu, Y. H.; Igarashi, Y.; Kodama, T.; Yamazaki, K.; Kyogoku, Y.; Kobayashi, Y. *Biochemistry* **1998**, *37*, 9641−9649.
(72) Timkovich, R.; Bergmann, D.; Arciero, D. M.; Hooper, A. B. *Biophys. J.* **1998**, *75*, 1964−1972.
(73) Reddy, K. S.; Angiolillo, P. J.; Wright, W. W.; Laberge, M.; Vanderkooi, J. M. *Biochemistry* **1996**, *35*, 12820−12830.
(74) Berry, E. A.; Trumpower, B. L. *Anal. Biochem.* **1987**, *161*, 1−15.
(75) Burns, P. D.; La Mar, G. N. *J. Biol. Chem.* **1981**, *256*, 4934−4939.

266 K and thus were excluded from this analysis). Despite the similar T_1 values at the two temperatures, the line widths of these methyls increase from 100 to 550 Hz as temperature is decreased from 298 to 266 K.

Discussion

We have expressed *Ne* cyt c_{552} from a synthetic gene and performed initial characterization of the product, NE. The UV−vis, CD, and NMR spectroscopic properties as well as the molecular mass of NE are consistent with expression of a well-folded nativelike product. Upon decrease of temperature to 266 from 298 K, the heme methyl resonances exhibit a small decrease in T_1 that cannot account for the large (∼5-fold) enhancement of line widths as temperature is lowered. This observation indicates that the temperature-dependent correlation time responsible for the line broadening is not the electronic relaxation time.[75] This finding is consistent with a greater contribution of chemical exchange to line widths as temperature is decreased, as might be caused by axial Met conformational fluxion as proposed for *Ht* cyt c_{552}.[6] If the axial Met in NE were to rapidly sample conformations such as those commonly displayed by other cytochromes shown in Figure 1A and B, the expected result is an "averaged" electronic structure, yielding a highly compressed heme methyl shift range (Figure 3).[6] Line broadening from exchange not involving the axial Met has been noted for ferricyt's *c*; however, in those cases only one methyl was affected.[75] Line broadening of all four methyls is consistent with dynamics of an axial ligand. Notably, the detailed analysis of reduced *Ne* cyt c_{552} structure by NMR spectroscopy indicates a single Met conformation.[72] It is possible that an oxidation-state-dependent change in the protein occurs, leading to conformational exchange in the oxidized state only. Further investigation is required to test this hypothesis.

Ligand fluxionality thus might be a more general phenomenon among heme proteins (and metalloproteins), rather than an anomaly displayed by the thermophilic *Ht* cyt c_{552}. For example, *Desulfovibrio vulgaris* Hildenborough cyt c_{553} has a compressed heme methyl shift range,[76] which also might indicate ligand dynamics. The possibility of the sampling of multiple ligand conformations should be considered in any metalloprotein, but might be particularly important in cases where sulfur serves as a donor to a metal. The structural basis for the ligand dynamics in NE and in *Ht* cyt c_{552} and the consequences for protein folding and function remain exciting targets of investigation. The ability to produce mutants of *Ne* cyt c_{552} and related proteins will be an important facility to be exploited in addressing these questions. In addition, the relationship between backbone and side-chain dynamics is of interest for future studies of these proteins. For example, it has not yet been determined whether proteins with axial Met side-chain fluxion also exhibit enhanced backbone dynamics. It also will be informative to learn whether mutations that alter side-chain dynamics also influence backbone dynamics. In reduced cyt's *c*, further studies of this phenomenon might be possible as axial Met side chain dynamics can be probed via ^{13}C relaxation experiments.[77] This approach will provide information important for understanding relationships between protein structure and dynamics in general.

Conclusions

The application of NMR spectroscopy to investigate cyt *c* folding and dynamics has answered many questions and also revealed areas in need of exploration. Future studies of folded-state dynamics of a wide variety of cyt's *c*, in combination with other biophysical and functional studies, are expected to provide data useful for understanding the complex interplay between protein structure, folding, dynamics, and function. The questions of how axial ligand conformations and fluctuations affect redox potential, reorganization energy for electron transfer, and electron-transfer pathway have not been satisfactorily explored. Studies of nonnative states of cyt's *c* also remain of interest. In particular, the biological consequences, if any, of in vivo cyt *c* unfolding and heme ligand switching, as can occur in the presence of membranes,[66,78] demands further study. Although cyt's *c* constitute one of the most well-studied protein families, much remains to be learned about their folding and dynamics. NMR spectroscopy promises to remain a vital tool for these continuing studies.

Experimental Section

Protein Expression and Purification. Molecular biology procedures were carried out generally as described previously.[79] The *Ne* cyt c_{552} gene was synthesized by Bionexus Inc. The plasmid pEC86 (Cm^r)[26] was a gift from Dr. Linda Thöny-Meyer. Restriction and DNA-modifying enzymes were purchased from Promega or Invitrogen. *E. coli* strain Nova Blue (Novagen) was used for cloning and ligation steps. *E. coli* strain BL21(DE3)-Star (Novagen) was used for protein expression. Oligonucleotide primer synthesis and DNA sequencing were performed at the University of Rochester Core Nucleic Acid Laboratory.

A gene encoding the *Ne* cyt c_{552} sequence was designed, optimizing *E. coli* codon usage, and was flanked with a 5′ *Nar*I restriction site and a 3′ *BamH*I restriction site. Immediately after the *Nar*I site are the codons for the first two amino acids of the mature *Ne* cyt c_{552} sequence. The synthetic gene was subcloned into the *Nar*I−*BamH*I site of pSCH552 (Amp^r),[25] placing the gene immediately at the end of a modified translocation sequence derived from *T. versutus* cyt c_{552}, the last two codons of which constitute the *Nar*I site.[34,80] DNA sequencing verified the expected gene sequence. The resulting plasmid is denoted pSNEC.

To express *Ne* cyt c_{552}, *E. coli* strain BL21(DE3)-Star-containing plasmids pSNEC and pEC86 were used to innoculate 250 mL of LB medium supplemented with 50 μg/mL ampicillin and chloramphenicol. The culture was shaken at 150 rpm, 37 °C, for 14 h and

(76) Senn, H.; Augster, A.; Wüthrich, K. *Biochim. Biophys. Acta* **1983**, *743*, 58−68.
(77) Flynn, P. F.; Urbauer, R. J. B.; Zhang, H.; Lee, A. L.; Wand, A. J. *Biochemistry* **2001**, *40*, 6559−6569.
(78) Pinheiro, T. J. T. *Biochimie* **1994**, *76*, 489−500.
(79) Sambrook, J.; Fritsch, E. F.; Maniatis, T. *Molecular Cloning: A Laboratory Manual*, 2nd ed.; Cold Spring Harbor Laboratory Press: Cold Spring Harbor, NY, 1989.
(80) Ubbink, M.; VanBeeumen, J.; Canters, G. W. *J. Bacteriol.* **1992**, *174*, 3707−3714.

then used to inoculate 1 L of LB medium supplemented with antibiotics in a 4-L flask, which was shaken for 18 h at 100 rpm, 37 °C. Cells were harvested by centrifugation (5000*g*, 10 min, 4 °C), yielding a dark pink cell pellet. The cell paste was frozen, thawed, and resuspended in lysis buffer [10 mM Tris-HCl, pH 7.0, 4 mg/mL lysozyme (25 mL per 1 L culture)] and incubated for 1 h at 30 °C. The mixture was centrifuged at 10000*g* for 15 min at 4 °C. The pink supernatant was loaded onto CM Sepharose Fast Flow ion-exchange resin (Amersham Pharmacia Biotech) equilibrated with 10 mM sodium acetate, pH 4.5, and eluted with a 0−180 mM NaCl gradient. The pink fraction was collected and concentrated using an Amicon ultrafiltration device with an YM-3 membrane (Millipore) and exchanged into 10 mM sodium acetate, pH 4.5, using a PD-10 column (Amersham Pharmacia Biotech). The product was oxidized overnight with a 10-fold excess of K[Co(EDTA)] (prepared as described elsewhere[81]) and subjected to a final purification step by FPLC using a Mono-S 10/10 column (Amersham Pharmacia Biotech). The protein was eluted with a 0−180 mM NaCl gradient in 10 mM NaOAc, pH 4.5.

Characterization of Recombinant *Ne* Cyt c_{552}. MALDI-TOF mass spectrometry was run in the reflector mode on a Voyager STR MALDI-TOF mass spectrometer. Protein samples were in H_2O, and the matrix used was sinnapinic acid (10 mg/mL of 50% acetonitrile plus 0.1% trifluoroacetic acid).

Absorption measurements were taken on a Shimadzu UV-2401PC photometer unit at room temperature. The spectra were recorded for both oxidized (as purified) and reduced (slight excess of dithionite added) species. The pyridine hemochrome was prepared as described.[74]

CD spectra were collected on an AVIV model 202 instrument with a jacketed cell holder connected to a circulating water bath. Protein samples (~10 μM) were in 50 mM sodium phosphate, pH 7.0, in 0.1-cm-path-length cells. Spectra were collected from 190 to 240 nm.

Proton NMR spectra were collected on a Varian INOVA 500-MHz spectrometer. Oxidized NE samples (1.0−1.4 mM) were in 50 mM sodium phosphate, pH 7.0, 10% D_2O, with a 5-fold molar excess of $K_3Fe(CN)_6$. Samples of reduced protein were purged with nitrogen prior to the addition of excess sodium dithionite. For observation of spectra at low temperature, samples in 50 mM sodium phosphate in D_2O, uncorrected pH 7.0, with 20% v/v CD_3OD and a 5-fold molar excess of $K_3Fe(CN)_6$ were prepared. 1-D NMR spectra were collected with 250-ms recycle times, and presaturation was used to suppress the solvent signal. T_1 measurements were made by the standard $180°-\tau-90°$ pulse sequence, with a 3-s recycle time.

Acknowledgment. This work was supported by a grant from the National Institutes of Health (GM63170) and an Alfred P. Sloan Research Fellowship to K.L.B. The authors thank Dr. James A. Fee for a productive collaboration on the *Tt* cyt c_{552} project and Dr. Linda Thöny-Meyer for the generous gift of pEC86. We also thank Terry Rabinowitz, Timur Senguen, and Lea Vacca for many stimulating discussions.

Supporting Information Available: Spectroscopic data (UV−vis, CD, NMR) used to characterize NE. This material is available free of charge via the Internet at http://pubs.acs.org.

IC048925T

(81) Dwyer, F. P.; Gyarfas, E. C.; Mellor, D. P. *J. Phys. Chem.* **1955**, *59*, 296−297.
(82) Bushnell, G. W.; Louie, G. V.; Brayer, G. D. *J. Mol. Biol.* **1990**, *214*, 585−595.
(83) Than, M. E.; Hof, P.; Huber, R.; Bourenkov, G. P.; Bartunik, H. D.; Buse, G.; Soulimane, T. *J. Mol. Biol.* **1997**, *271*, 629−644.
(84) Kraulis, P. J. *J. App. Cryst.* **1991**, *24*, 946−950.
(85) (a) Keller, R. M.; Wüthrich, K. *Biochem. Biophys. Res. Commun.* **1978**, *83*, 1132−1139. (b) Timkovich, R. *Inorg. Chem.* **1991**, *30*, 37−42.
(86) Keller, R. M.; Wüthrich, K. *Biochim. Biophys. Acta* **1978**, *533*, 195−208.
(87) (a) Feng, Y.; Roder, H.; Englander, S. W. *Biochemistry* **1990**, *29*, 3494−3504. (b) Timkovich, R.; Cai, M. *Biochemistry* **1993**, *32*, 11516−11523.